UNIVERSITY OF MICHIGAN
ENGINEERING RESEARCH INSTITUTE

ELECTRONIC DEFENSE GROUP TECHNICAL MEMORANDUM NO. 12

SUBJECT: Report on Induced Grid Noise Measurements

BY: T. E. Talpey

DATE: July 16, 1953

Introduction

This report contains a description of the method used to measure induced grid noise, a table showing typical magnitudes of noise likely to be found in modern miniature receiving tubes and a discussion of the application of this data to the design of low-noise amplifiers. In addition, a description is included (with photographs) of equipment constructed for the measurement of noise at 30 mc.

With the exception of a few minor changes and the addition of some data to Table I, this report is identical with Chapter IV and Appendices II and III of a thesis written by the author.* The bibliography of the complete thesis is included for convenience, although only a few of the references are cited in this report.

1. Method of Measurement

The most convenient method of measuring fluctuation noise at the frequencies employed in this study (30 mc.) is the use of a comparator diode: the noise to be measured is compared with the shot noise of a temperature-limited diode. Fig. 1.1 presents a block diagram of the

---

* "A Study of Induced Grid Noise" by T.E. Talpey. This thesis was submitted by the author to the University of Michigan in partial fulfillment of the requirements for the Ph.D. degree in electrical engineering and is available on microfilm.

apparatus employed and Section 4 contains a detailed description of the actual equipment.

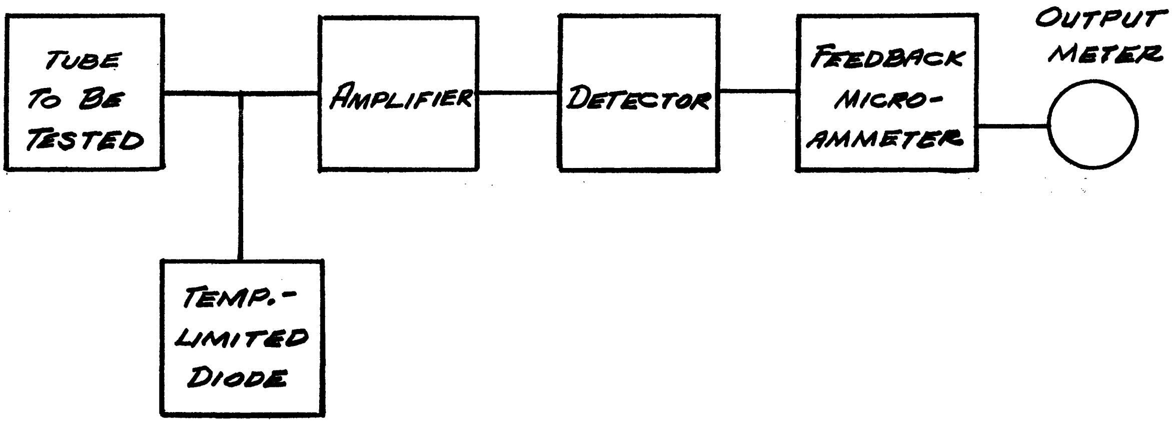

Figure 1.1. Block diagram of the apparatus used for noise measurements.

The tube to be tested (in this case the grid of the tube to be tested) is connected to the input of a high-gain, low-noise amplifier, with a very narrow bandwidth. The plate of the noise diode is also connected to the amplifier input terminals. The fluctuation currents produced by these two tubes flow through the input circuit of the amplifier and produce noise voltages which are then amplified and detected, the response of the detector giving an indication of the amount of noise present at the amplifier input. The actual process of comparing the diode shot noise with the noise to be measured is complicated somewhat by the fact that the amplifier contains several additional sources of noise which must be taken into account. Before developing the equations employed in computing the unknown noise of the tube under test, a few remarks are necessary concerning the overall characteristics of the measuring system.

It is known[9] that the mean square noise current generated by a temperature-limited diode is given accurately by the following equation:

$$\overline{i^2} = 2eI\Delta f \qquad (1.1)$$

up to frequencies at which the transit angle of the diode approaches one radian. The measurements reported here were made at a frequency of 30 mc., for which the diode transit angle is only about one-tenth of a radian. In Eq (1.1), e is the change on an electron, I is the d.c. current of the diode, and Δf is the bandwidth.

The detector used for these measurements was a crystal operating at a very low level (below one micro-ampere), and it was expected that its characteristic would be very nearly square-law; Eq (1.1) tells us that if the amplifier is linear we can expect a plot of crystal current vs. diode plate current to be a straight line. This provides us with an accurate check on the operation of the complete system, including the microammeter used to measure crystal current. Fig. 4.9 of Section 4 shows that we are completely justified in assuming that the reading of our output meter is linearly related to the mean square fluctuation current flowing through the input circuit of the amplifier.

The basic principle by which measurements are made of the unknown noise of a tube under test is as follows: The increase in the reading of the output meter is noted when the source of noise to be measured is turned on. The unknown noise is then turned off and the diode turned on and adjusted so that it produces the same increase in output. The diode plate current, through Eq (1.1), then gives us a measure of the noise current introduced into the circuit by the tube under test. Unfortunately, this process has to be modified slightly because of the fact that changes in the admittance of the input circuit occur as the tube under test is turned on and off.

In order to develope a quantitative relationship for the unknown noise of the tube under test it is necessary to consider in detail the input circuit of the amplifier and the noise sources connected to it. Fig. 1.2 shows the equivalent r.f. circuit at the input terminals of the amplifier, the various noise sources being represented by current and voltage generators. The following notation has been used:

$\overline{i_t^2}$ = mean square noise current introduced into the circuit by the tube being tested,

G_t = conductance added to the circuit when the tube under test is allowed to draw plate current,

$\overline{i_d^2}$ = mean square noise current produced by the temperature-limited diode

$= 2eI\Delta f$

$\overline{i_c^2}$ = mean square noise current produced by the input circuit conductance,

G_g = conductance produced by transit-time loading at the grid of the input tube of the amplifier,

$\overline{e_{eq}^2}$ = mean square noise voltage representing the effect of shot noise at the plate of the input tube of the amplifier

$$= 4kTR_{eq}\Delta f = \frac{2eI_b\Gamma^2\Delta f}{gm^2} .$$

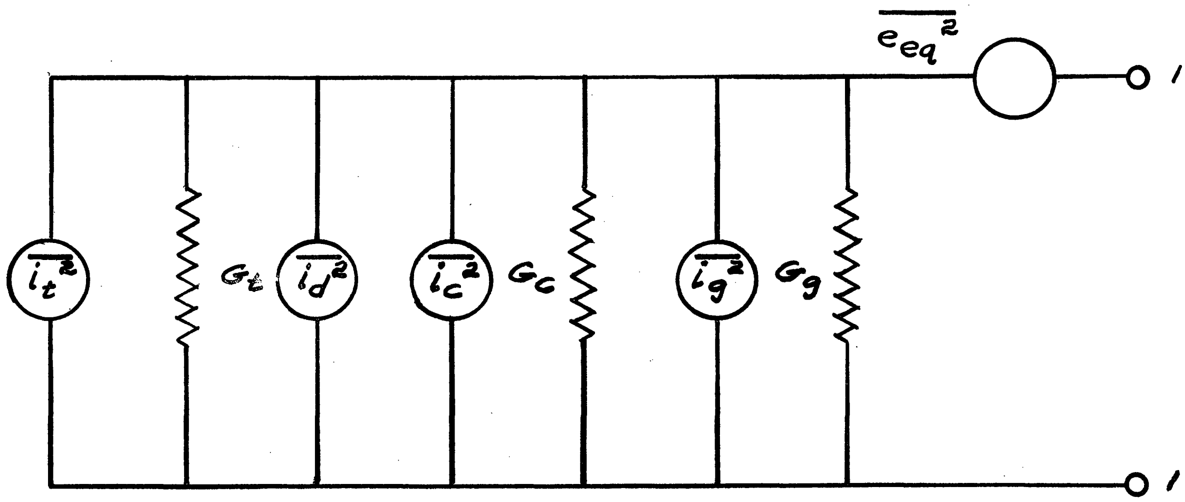

Figure 1.2. Equivalent r.f. circuit of the amplifier input.

The noise voltage appearing at terminals 1 - 1 is amplified by the system and the output of the crystal detector is proportional to $\overline{e_{11}^2}$, that is:

$$K \cdot I_{out} = \overline{e_{11}^2} . \qquad (1.2)$$

This equality is based on the assumption, discussed above, that the over-all system has a square-law characteristic. Noise coming from other sources in the amplifier has been neglected as it is very small and also would be found to cancel out in the derivation which follows.

With the amplifier operating alone (diode turned off, tube under test biased beyond cut-off) the reading of the output meter, I_1, is given by the following expression:

$$K \cdot I_1 = \overline{e_{11}^2} = (\overline{i_c^2} + \overline{i_g^2})(G_c + G_g)^2 + e_{eq}^2. \qquad (1.3)$$

The voltages are added by their squares since the noise sources are independent of each other, with the exception of one component of $\overline{i_g^2}$ which is in quadrature with $\overline{e_{eq}^2}$ and hence adds as a square also. It is assumed in writing Eq (1.3) as well as the equations to follow that the input circuit is tuned so that there is no susceptive component in the input admittance. This is accomplished by peaking the output by means of a small variable capacitor connected in parallel with the input circuit. Actually this adjustment is not too critical because the bandwidth of the input circuit is much greater than the remainder of the amplifier.

With the amplifier and the diode operating, but with the tube under test still biased beyond cut-off, the reading of the output meter, I_2, is given by:

$$K \cdot I_2 = \overline{e_{11}^2} = (\overline{i_c^2} + \overline{i_g^2} + 2eI\Delta f)\ (G_c + G_g)^2 + \overline{e_{eq}^2}. \quad (1.4)$$

When the diode is in operation, a small additional conductance is introduced in parallel with G_c and G_g, but this added conductance is so small compared with the sum $(G_c + G_g)$ that it can be neglected.

When the diode is turned off and the tube under test is turned on, the output becomes:

$$K \cdot I_3 = (\overline{i_c^2} + \overline{i_g^2} + \overline{i_t^2})\ (G_c + G_g + G_t)^2 + \overline{e_{eq}^2}. \quad (1.5)$$

The operation of the tube under test introduces a conductance G_t which usually cannot be neglected. A change in the input tuning capacitance is also necessary because of the change in input capacitance of the tube under test when its grid bias is changed. The bandwidth of the input circuit is also changed somewhat by the addition of G_t, but since the bandwidth of the remainder of the amplifier is so much narrower, this change does not appreciably alter the overall bandwidth of the system.

Finally, with the complete circuit in operation, tube under test, diode and amplifier turned on, the output becomes:

$$K \cdot I_4 = (\overline{i_c^2} + \overline{i_g^2} + \overline{i_t^2} + 2eI'\Delta f)\ (G_c + G_g + G_t)^2 + \overline{e_{eq}^2}. \quad (1.6)$$

It is convenient to carry out the measurement procedure in such a way as to make $I_4 = 2I_3$ and $I_2 = 2I_1$. This makes the diode current I' in Eq (1.6) greater than the current I in Eq (1.4). The difference (I' - I) is denoted by ΔI. The simultaneous solution of Eqs (1.3) to (1.6), plus the substitution of the equation for $\overline{e_{eq}^2}$, enables us to obtain the unknown noise current $\overline{i_t^2}$, and the unknown conductance G_t, in terms of ΔI and several other easily measured quantities. We thus obtain the formulas necessary for the experimental testing of tubes:

$$i_t^2 = 2e(\Delta I)\ (\Delta f) + 4kTR_{eq}(G_c + G_g)^2(1 - \rho) \quad (1.7)$$

$$G_t = (G_c + G_g)\ \frac{1 - \rho}{1. + \sqrt{\rho}} \quad (1.8)$$

where

$$\rho = \frac{I_1}{I_3} \times \frac{I'}{I}\ . \quad (1.9)$$

The second term on the right in Eq (1.7) is considerably smaller than the first and can be considered essentially a correction term. When the unknown fluctuation current is realtively large, as for example when measurements are made of shot noise, this correction term can be neglected entirely. For the measurement of grid noise, however, it is usually necessary to include it. In computing its magnitude the quantity ρ is obtained from experimental data, the factor $(G_c + G_g)$ is easily measured with a high-frequency bridge, and R_{eq} can be estimated (or measured) with accuracy sufficient for such a correction term.

It must be remarked that the measured input conductance, G_t, of the tube under test cannot be taken to be the input damping due to transit time effects. Small residual inductances in the leads of the tube together with inter-electrode capacitances cause the total input conductance to be greater than that due to transit time alone. Fortunately, these lead inductances have negligible effect on grid noise so that Eq (1.7) still remains valid. Bakker[3] discusses the justification for neglecting the effect of lead inductance on induced grid noise and it is discussed quantitatively in Section 5 of this report. The point to be made here is that the application of Eq (1.7) will enable us to determine the noise current induced in the grid circuit by the tube under test, but that Eq (1.8) will not yield the correct value of transit-time conductance. The separation of total input conductance into components due to transit time and lead inductance effects is not a simple task. The reader is referred to a paper by Strutt and van der Ziel[49] for a discussion of this problem.

2. Measured Values of Induced Grid Noise

In presenting the results of the measurements outlined in Section 1.1 we are forced to choose between a direct presentation of $\overline{i_t^2}$, which has the advantage of clarity, and an indirect specification of, for example, an equivalent noise temperature or an equivalent noise conductance, which are more convenient from a design engineer's point of view. Many articles in the literature concerned with grid noise specify the equivalent plate current of a temperature-limited diode which would produce a fluctuation current equal to $\overline{i_t^2}$. This seems to the author to be a fairly good compromise between the two points of view. The theoreticians need simply multiply the equivalent diode current by $2e\Delta f$ to obtain $\overline{i_t^2}$ and the design engineer can use the factor $\frac{e}{2kT}$ to obtain the equivalent noise conductance. The factor $\frac{e}{2kT}$ is approximately equal to 20 for normal room temperature.

It should be emphasized that the equivalent grid-noise conductance is not the same as the transit-time conductance which loads the input circuit. The ratio of equivalent grid-noise conductance to transit-time conductance is equal to the ratio of equivalent grid-noise temperature to room temperature. For many engineering design problems this ratio can be taken roughly as five. (Cf. North and Ferris[5])

For reasons outlined above the value of each experimentally determined mean square grid noise current is presented here in terms of an equivalent temperature-limited diode current, denoted by I_d. It is calculated by dividing Eq (1.7) by $2e\Delta f$, giving:

$$I_d = \Delta I + \frac{R_{eq}}{20}(G_c + G_g)^2(1 - \rho). \qquad (2.1)$$

A summary of measurements made of the induced grid noise of several miniature tubes is presented in Table I. In come cases it was possible to measure a great many tubes of a given type; for other types only a few tubes were compared. The number of tubes examined, the average grid noise, the lowest and highest noise found in each group, the plate current at which the noise was measured and the (measured) equivalent shot noise resistance are shown for each tube type. All the measurements shown were made with a plate voltage of 150 volts and at a frequency of 30 mc. All the tubes were connected as triodes.

In addition there is a column in Table I labeled "F_{opt}", indicating the lowest noise factor obtainable at 30 mc. from the average tube under the conditions of plate voltage and plate current shown. As discussed in the next section it may be possible to obtain a lower noise factor by the use of a different combination of plate voltage, grid bias and plate current. However, the last column of Table I gives us a means of judging the merits of each tube for use in a low-noise amplifier.

The method used in obtaining "F_{opt}" in Table I is as follows: For the low-noise cascode amplifier it has been shown[2] that the optimum value of source resistance, giving the lowest noise factor, is given approximately by:

$$R_{s_{opt}} \cong \frac{1}{g_m} \sqrt{\frac{\overline{i_p^2}}{\overline{i_g^2}}} \quad . \tag{2.2}$$

The use of a source resistance of this amount leads to an optimum noise factor

$$F_{opt} = 1 + \frac{\sqrt{\overline{i_p^2} \cdot \overline{i_g^2}}}{2kT \quad f g_m} \quad . \tag{2.3}$$

The factor $\frac{\sqrt{\overline{i_p^2} \cdot \overline{i_g^2}}}{g_m}$ might be called a figure of merit for the tube with respect to its noise factor. The lower this ratio the lower the noise factor can be made. This gives us a basis for comparing tubes as to their performance in a low-noise cascode amplifier. In drawing up Table I measured values of $\overline{i_p^2}$, $\overline{i_g^2}$ and g_m of a tube fitting the "average" column were used in conjunction with Eq (2.3).

A few remarks are necessary concerning the accuracy of the data in Table I. The equivalent diode currents were obtained essentially by

TABLE I

MEASURED VALUES OF INDUCED GRID NOISE AT 30 mc.

Tube Type	Number Examined	Induced Grid Noise Equivalent diode current I_d, in microamperes Average	Lowest	Highest	Plate Current I_b in ma.	Equivalent Shot Noise Resistance R_{eq}	Transconductance g_m in micromhos	F_{opt}
6AG5	21	7.1	5.6	7.8	7	480	6000	1.52
6AK5	30	2.3	1.8	2.9	10	460	5500	1.29
6AS6*	4	2.3	2.1	2.6	10	450	5800	1.29
6AU6	17	10.6	9.2	12.7	12	420	6600	1.60
6BC5	6	6.5	6.0	7.1	8	590	5800	1.56
6BH6*	3	11.2	—	—	10	—	—	—
6CB6*	10	8.7	7.2	9.7	12	410	7300	1.54
6J4	2	10.0	—	—	15	321	12,000	1.51
6J6**	10	3.0	2.1	4.1	8	720	4400	1.42
2C51**	8	2.0	1.9	2.3	8	550	5400	1.30
404A	9	3.6	3.4	1.8	15	240	16,000	1.27

* Suppressor Connected to plate and screen.

** Values are for a single section.

Caution: The values given in this table, while representative, should not be considered universal. When measurements are taken on only a few tubes of each type, it is quite possible that the average of such a small number may not represent a ture average of overall production.

measuring the difference, ΔI, between two diode currents. In many cases this difference was rather small, amounting to two or three microamperes out of about fifteen or twenty. The meter used to measure these currents was carefully calibrated beforehand to an accuracy as close as the scale could be read, 0.1 microampere. Taking the worst possible cases, where the meter reading was in error by 0.1 microampere in one direction for the first reading and the same amount in the other direction for the second reading, the possible error in ΔI would be 0.2 microampere. This would lead to an error of 10 percent for an equivalent diode current of 2.0 microamperes. The errors in Table I from this source are less than this amount, however, for the data presented here represent averages of a number of measurements on each tube. In addition, for most tubes the value of ΔI is larger than that assumed in the above calculation, making the percent error smaller.

Besides the error introduced by uncertainties in the readings of the diode plate current meter there is an uncertainty of about the same order of magnitude in the setting of the output current to double its original value. In order to apply Eqs (1.7) to (1.9) it is necessary to make $I_2 = 2I_1$ and $I_4 = 2I_3$, as discussed in Section 1.1. Our inability to do this exactly results in an additional source of error. We are aided somewhat in this respect by the construction of the microammeter: the range of the microammeter is changed by a factor of two by the same switch that turns on the noise-diode plate voltage. We are then able to adjust the diode current until the needle of the output meter rests at exactly the same spot on its scale while the diode is turned off and on and the microammeter range simultaneously switched from 1.0 to 0.5 microamperes. This procedure increases considerably the accuracy with which we are able to obtain the conditions $I_2 = 2I_1$, etc.

The amount of error introduced by the attenuator associated with the range switch mentioned above is well below the magnitudes of the errors which have just been considered. The errors coming from non-linearity of the measurement apparatus are likewise much smaller than those arising from the reading of meters. (See Fig. 4.9 of Section 4)

Taking into account all of the above considerations it is estimated that the probable error in the data of the "average" column of Table I ranges from about 10 percent for those tubes having small values of induced grid noise to less than 5 percent for those tubes having a large amount of grid noise. This is well within the limits of variability indicated in Table I for all tube types and hence entirely adequate for design purposes. Any given tube may easily vary from the values given here by more than twice the probable error of the data in Table I.

The variability between tubes of a given type is indicated by the "lowest" and "highest" columns of Table I. This variability is caused for the most part by slight differences in electrode spacings, alignment of grids, etc. A few tubes were found to have abnormally high grid noise due to the presence of a small amount of gas (as indicated by a small ion current to the grid) but these tubes were not included in tabulating the data for Table I.

3. Application of Measured Grid Noise Values to Amplifier Design

Table I gives the value of induced grid noise to be expected from each tube type under the conditions of plate voltage and plate current specified in the table and at a frequency of 30 mc. The voltage and current have been chosen to give typical operating conditions but of course any given amplifier will probably not be operating at 30 mc. A method is required for extrapolating the data of Table I to other frequencies. Theory predicts and experiments[3] have shown that the mean square induced grid noise current varies as the square of frequency, as long as the transit angle is small. Thus to obtain the induced grid noise at any frequency we need only multiply the data in Table I by the square of the ratio of the new frequency to 30 mc. For example, the equivalent diode current for the grid noise of a 6AK5 at 100 mc. is $\frac{100}{30}^2 \times 2.3 = 25.5$ microamperes.

We may also wish to extend the data of Table I to other values of plate voltage and plate current. This cannot be done with anything like the accuracy of frequency extrapolation, but it is possible to make some general predictions. For example, if the grid bias is held constant (at the value giving the plate current in Table I at a plate voltage of 150 volts) then the induced grid noise will not change appreciably as the plate voltage is varied, unless the voltage is made abnormally low. This is illustrated by the lower curve in Fig. 3.1.

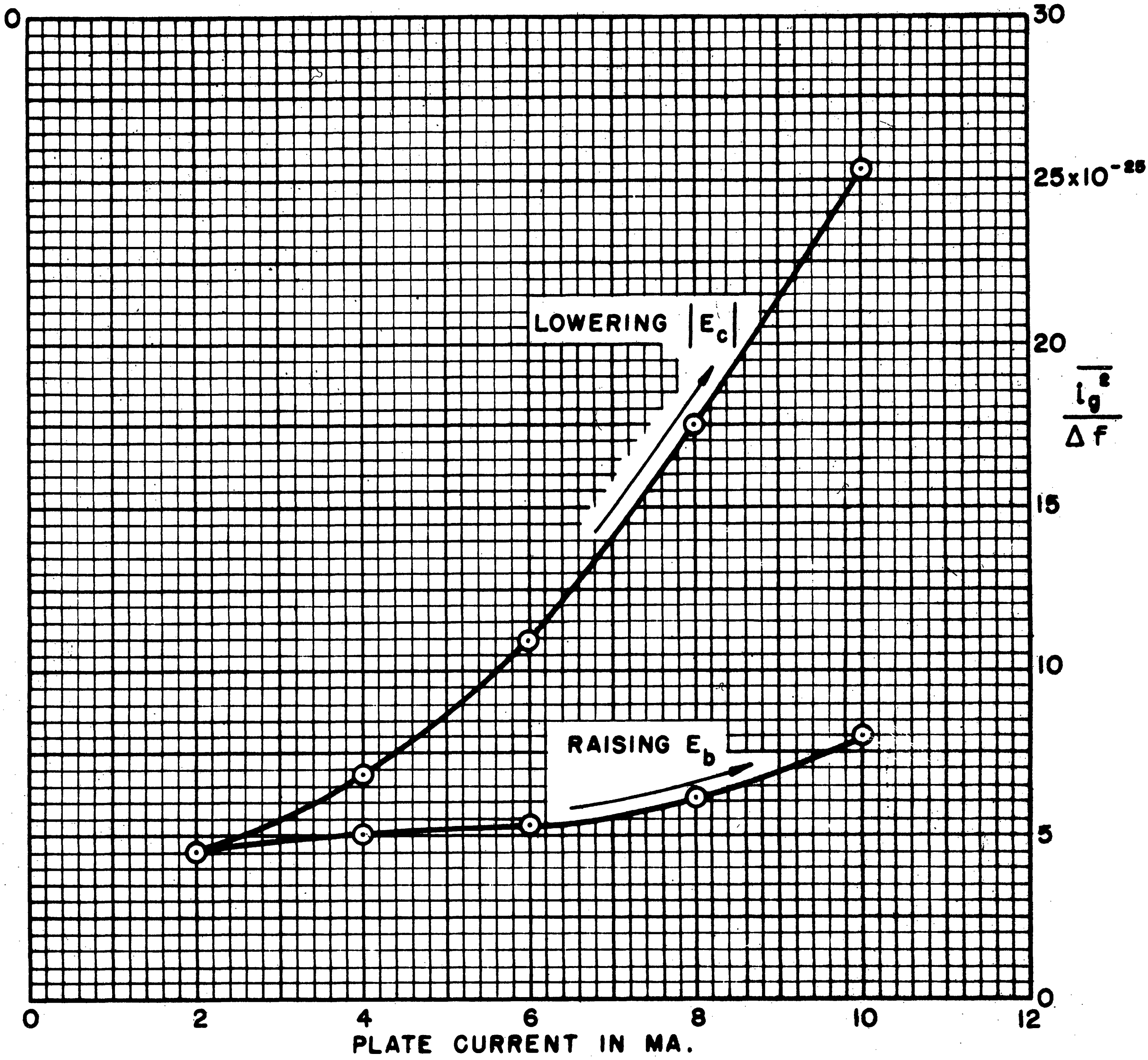

Figure 3.1. Mean square induced grid noise current in (amperes)^2 per cycle bandwidth vs. plate current for one-half of a 6J6 double triode at 30 mc.

Upper curve: I_b increased by reducing grid bias.

Lower curve: I_b increased by increasing plate voltage. E_c = -2.9 v, and E_b = 100 v for both curves at I_b = 2 ma.

If the grid bias and plate voltage are varied simultaneously in such a way as to hold the plate current constant, then the induced grid noise will decrease with increasingly negative grid biases, as shown in Fig. 3.2. The accurate prediction of the magnitude of this reduction is rather difficult and not of enough practical value to warrant a detailed study. Fig. 3.2 indicates that for a given plate current (or transconductance) the tube should be operated with as high a negative grid bias and as high a positive plate voltage as possible without exceeding the plate dissipation rating of the tube.

If the plate voltage is held constant and plate current varied by changing the grid bias a variation of grid noise similar to that shown in Fig. 3.3 a is observed. The same grid noise data is plotted vs. transconductance in Fig. 3.3 b.

The exact calculation of induced grid noise by extrapolation from a given point on one of these curves is not possible, because the curves are widely different from one tube to the next--the bends

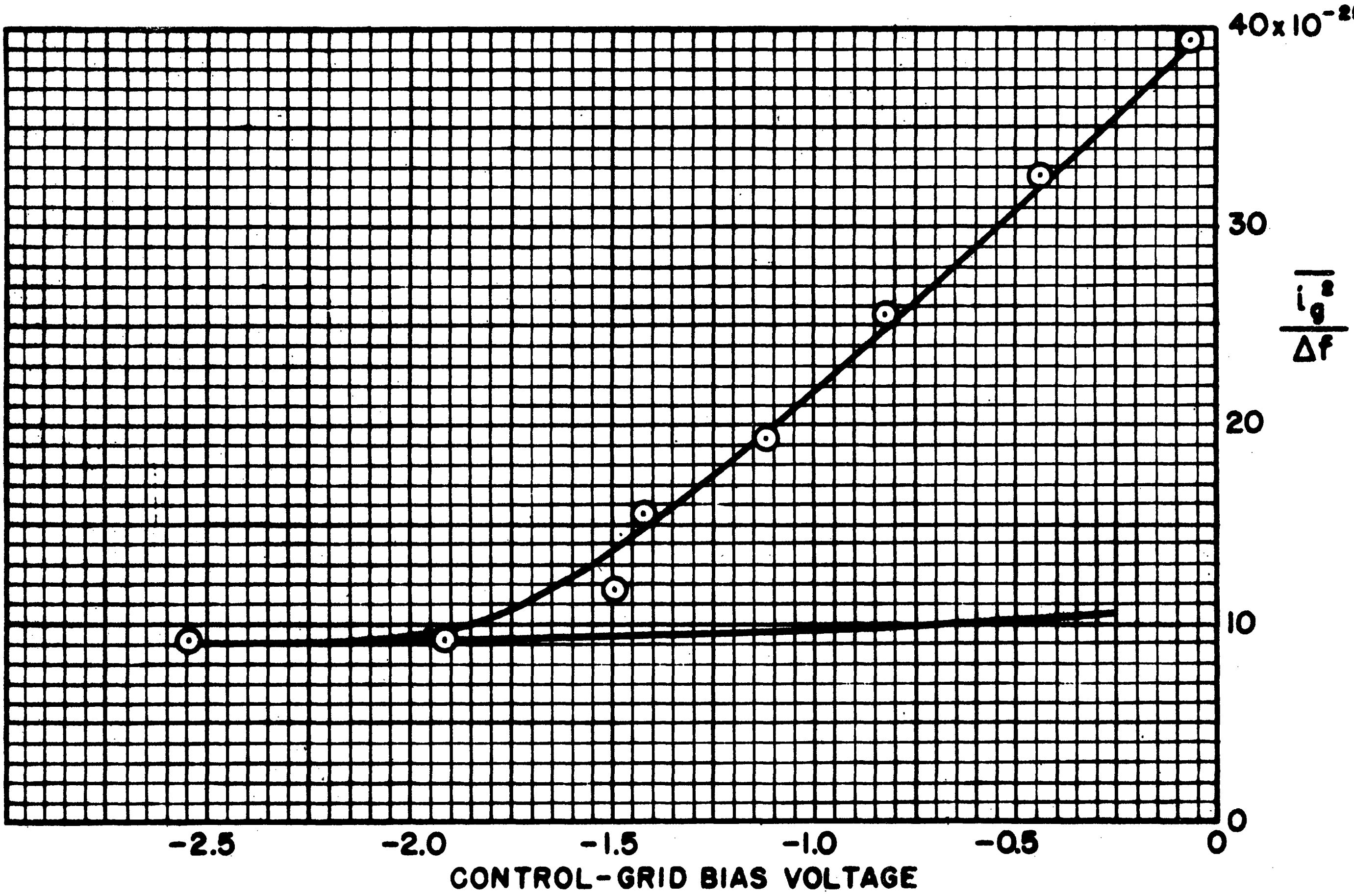

Figure 3.2. Upper curve: Experimental values of the mean square induced grid noise current in (amperes)^2 per cycle bandwidth vs. control-grid bias for one-half of a 6J6 double triode at 30 mc, with constant plate current of 8 ma. The values are corrected for shot noise in the dc grid current which occurred at low bias voltages. Lower curve: Values predicted on the basis of transit time theory, adjusted to match experiment at large negative biases.

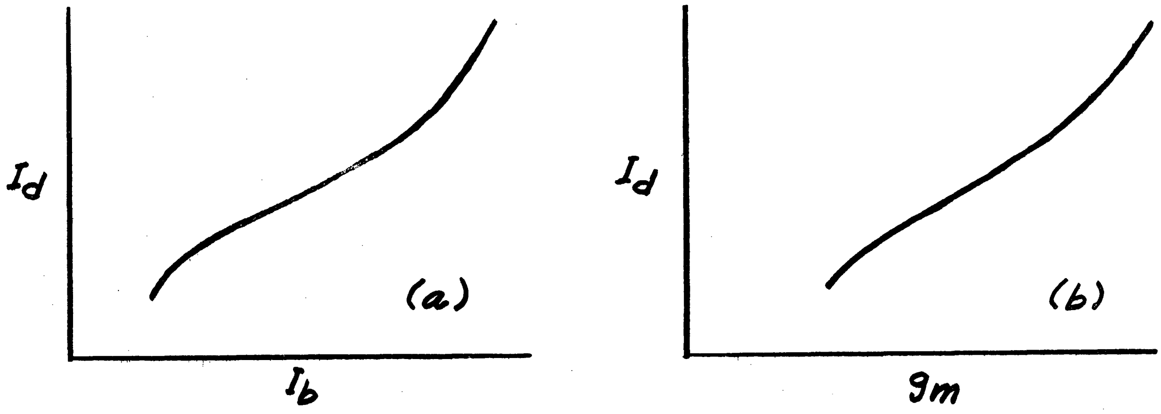

Figure 3.3. Typical plots of induced grid noise as a function of (a) plate current and (b) transconductance. The equivalent noise-diode currents (I_d) for these curves were taken from measurements of the induced grid noise of a 6J6 at 30 mc.

are in different places, slopes are not the same, etc. For some tubes the curve of I_d vs. g_m turns out to be nearly a straight line and in these cases it might be possible to make some sort of a rough linear extrapolation which would be sufficiently accurate. In the majority of cases, however, the most that can be said is that grid noise increases with g_m, although not linearly.

This fact has one important application in the design of low-noise amplifiers. It is sometimes stated* that the input tube of a low-noise amplifier should be operated with low grid bias and high plate current, in order to produce a high value of g_m. For some tubes, and at low frequencies, this statement is correct, but in many cases it leads to a poorer noise factor than the optimum obtainable from the tube under

---

* See, for example, page 637 of Reference 6.

proper operating conditions.. The reason for this is quite simple: as plate current is increased (by reducing grid bias) the equivalent shot noise resistance, $R_{eq} = \frac{2.5}{g_m}$, decreases and induced grid noise increases, as shown by Fig. 3.3. If induced grid noise should increase faster than R_{eq} decreases, then a deterioration of the amplifier noise factor may result. For a 6AK5 operating at 30 mc. the induced grid noise is too small to cause any appreciable deterioration but for most other tubes and for the 6AK5 at higher frequencies the effect on noise factor is by no means negligible.

Tests were made on the noise factor of a cascode amplifier at 30 mc. employing a triode-connected 6AG5 input tube. Curves of noise factor vs. source conductance were made for a number of different grid biases and from these curves the minimum obtainable noise factor was determined for each value of grid bias. Fig. 3.4 shows the results of these tests, indicating the undesirability of operating the tube at maximum plate current.

The conclusion to be drawn from the above discussion is that a reduction of grid bias and the consequent increase in g_m will not always reduce the noise factor of an amplifier. If the plate current and consequently g_m are increased by increasing the plate voltage,

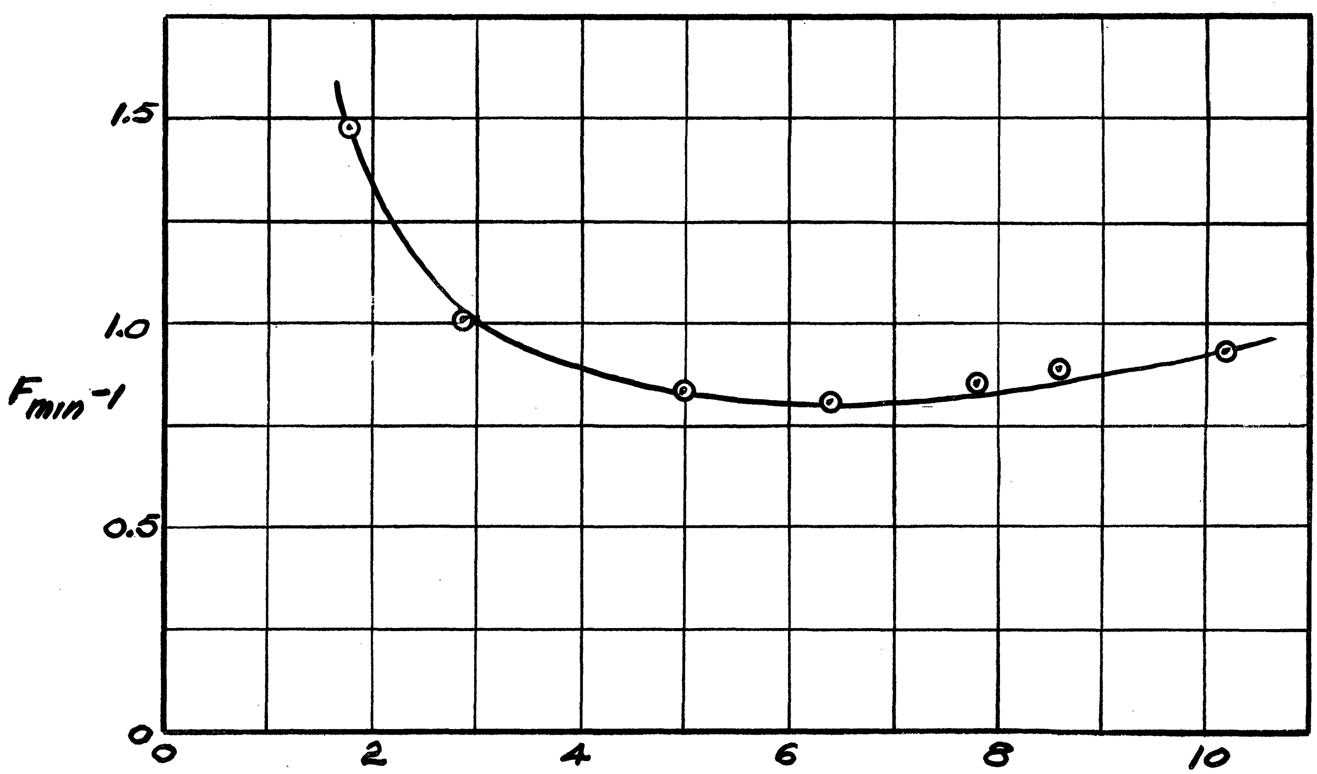

Plate Current, I_b, in Milliamperes

Figure 3.4. Minimum noise factor as a function of plate current for a 30 mc. cascode amplifier employing a triode-connected 6AG5 as the input tube.

leaving the grid bias unchanged, then as shown by Fig. 3.1, there will be relatively little increase in grid noise and a lower noise figure will be obtained because of the reduction in R_{eq}. For example, referring to Fig. 3.4, if the plate voltage were increased 50 volts or so, the minimum of the curve would shift to the right and down slightly provided the grid bias were left unchanged.

There appears to be an optimum combination of plate voltage and grid bias which will provide the lowest possible noise factor for an amplifier. Unfortunately it is not possible to specify these operating conditions precisely for they depend on characteristics of the circuit as well as the tube. Although the optimum operating point must ultimately be determined by trial and error, the above comments should be helpful in predicting which changes can be expected to lead to an improvement in noise factor. The reader is referred to References 2 and 6 for more complete discussions on the characteristics and design of low-noise amplifiers.

4. Description of the Measuring Equipment

This section presents descriptions and details of the circuits used in constructing the apparatus with which grid noise measurements were made. The circuit represented by each of the blocks in Fig. 1.1 is presented and discussed, and the unusual features in its design and construction are pointed out.

The circuit used to supply the required voltages to the tube under test is shown in Fig. 4.1. The terminal labeled "a" connects directly to the input of the amplifier described on succeeding pages. The heater connections are not shown--one side of the heater is connected to ground and the other connection is made through an r.f. filter to an adjustable source of heater voltage.

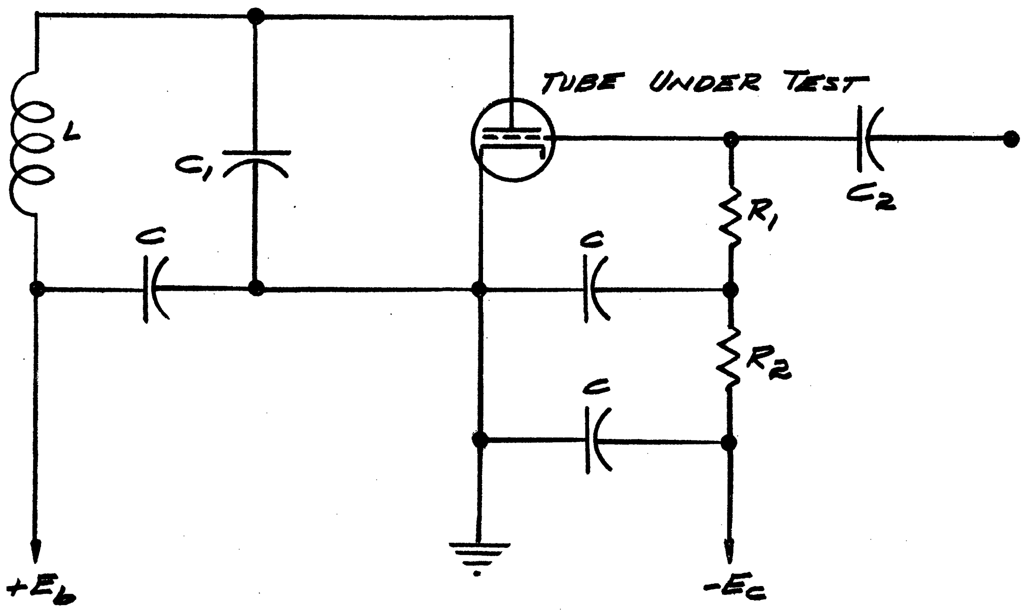

Figure 4.1. Circuit used to supply operating voltages to tube under test.

The capacitor C_1 was made series resonant with its leads (by adjusting the lead lengths) in order to provide as good an r.f. short-circuit as possible between plate and cathode. The capacitors labeled C are conventional by-pass capacitors (10000$\mu\mu$fd.). C_2 is the coupling capacitor to the amplifier input--its nominal value is 560 $\mu\mu$fd. All capacitors are of the ceramic type.

The inductance L is essentially an r.f. choke but it is wound so as to be self-resonant with its distributed capacitance at about 30 mc., thus increasing its impedance to r.f. currents. It is desirable to use a choke for the filter in the plate lead so that the plate voltage can be conveniently measured without connecting an additional lead directly to the plate.

It is not necessary to use an inductance in the filter to the grid lead because no d.c. current flows in this circuit. Indeed, it is desirable to avoid the use of an inductance in this filter, for no matter how carefully the plate and grid leads may be shielded there is always a possibility that a small amount of coupling could exist through the medium of a mutual inductance between the grid and plate chokes. In this event, any plate noise which succeeds in avoiding the by-pass capacitor C, would cause some additional noise in the grid circuit, leading to experimental errors.

The resistance R_1 loads the input circuit of the amplifier and its effect must be taken into account in determining the magnitude of the correction term in Eq (1.7). It should be of relatively high resistance to avoid unnecessary loading of the amplifier input.

The plate supply, E_b, and the grid bias supply, E_c, both contain milliammeters: one to measure plate current and the other to monitor the grid circuit for possible grid current which would be indicative of a gassy tube. Such a tube would have abnormally large grid noise.

Fig. 4.2 shows the circuit used for the standard noise generator. It is of conventional design and a complete description of the construction of a similar noise source can be found in Chapter 14 of Reference 6.

The plate of the noise diode (point "a") is connected directly to the input coil of the amplifier and the d.c. plate current of the diode flows through this coil. It is shown dotted in Fig. 4.2. The cathode of the diode is made negative with respect to ground since the plate is at d.c. ground potential. The diode (a Sylvania type 5722 noise diode) is operated temperature-limited and a simple measurement of its d.c. plate current enables us to determine the noise current added to the amplifier input circuit.

The filament current and hence the emission of the noise diode is varied by means of the resistance R in series with the filament supply battery. This is a storage battery and arrangements were made to put it on "trickle" charge when not in use for noise measurements. The use of a transformer for the filament supply was found to be unsatisfactory because

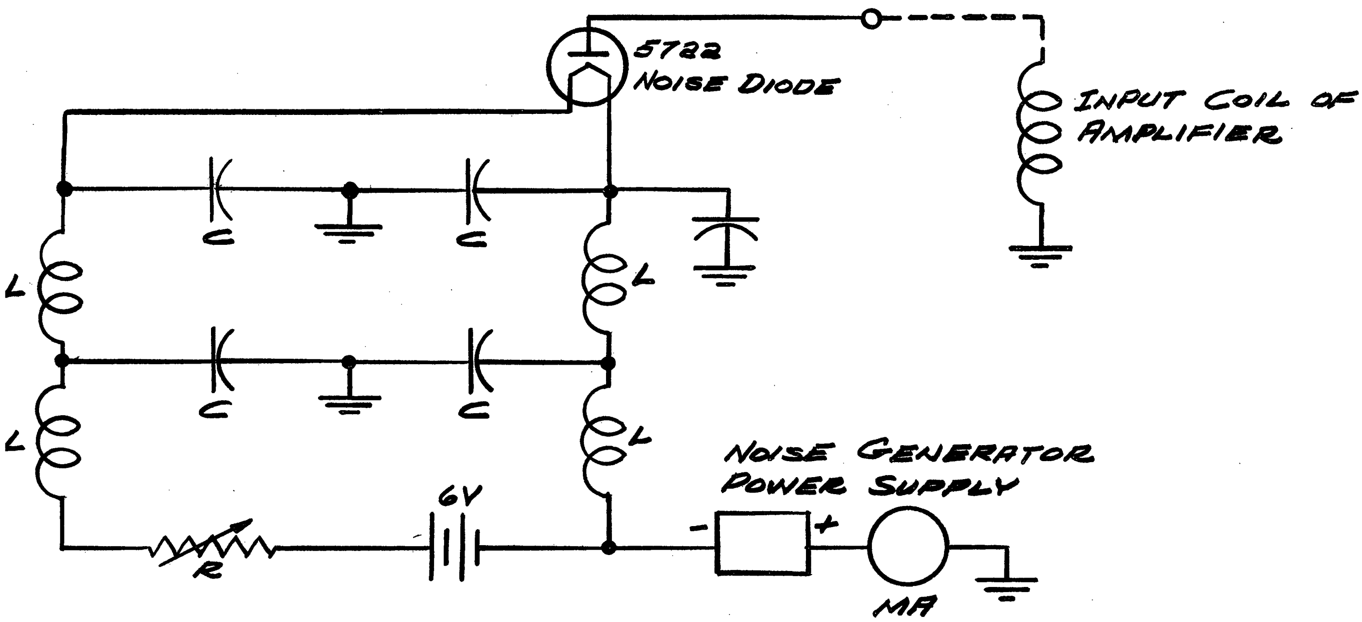

Figure 4.2. Circuit of the noise generator.

of variations in line voltage which could not be reduced sufficiently even when a constant voltage transformer was employed.

It is necessary to carefully shield the circuits of Figs. 4.1 and 4.2, as well as the input circuit of the amplifier to which they are connected. If even a slight amount of coupling should exist between the output of the amplifier and either of these circuits, regeneration could take place and produce disturbing effects on noise measurements.

Fig. 4.3 shows the shielding of the tube under test and the diode noise generator as well as the input circuit of the amplifier. The filters in the leads of the diode and the tube under test can be seen clearly and the input coil and neutralizing coil of the casode amplifier

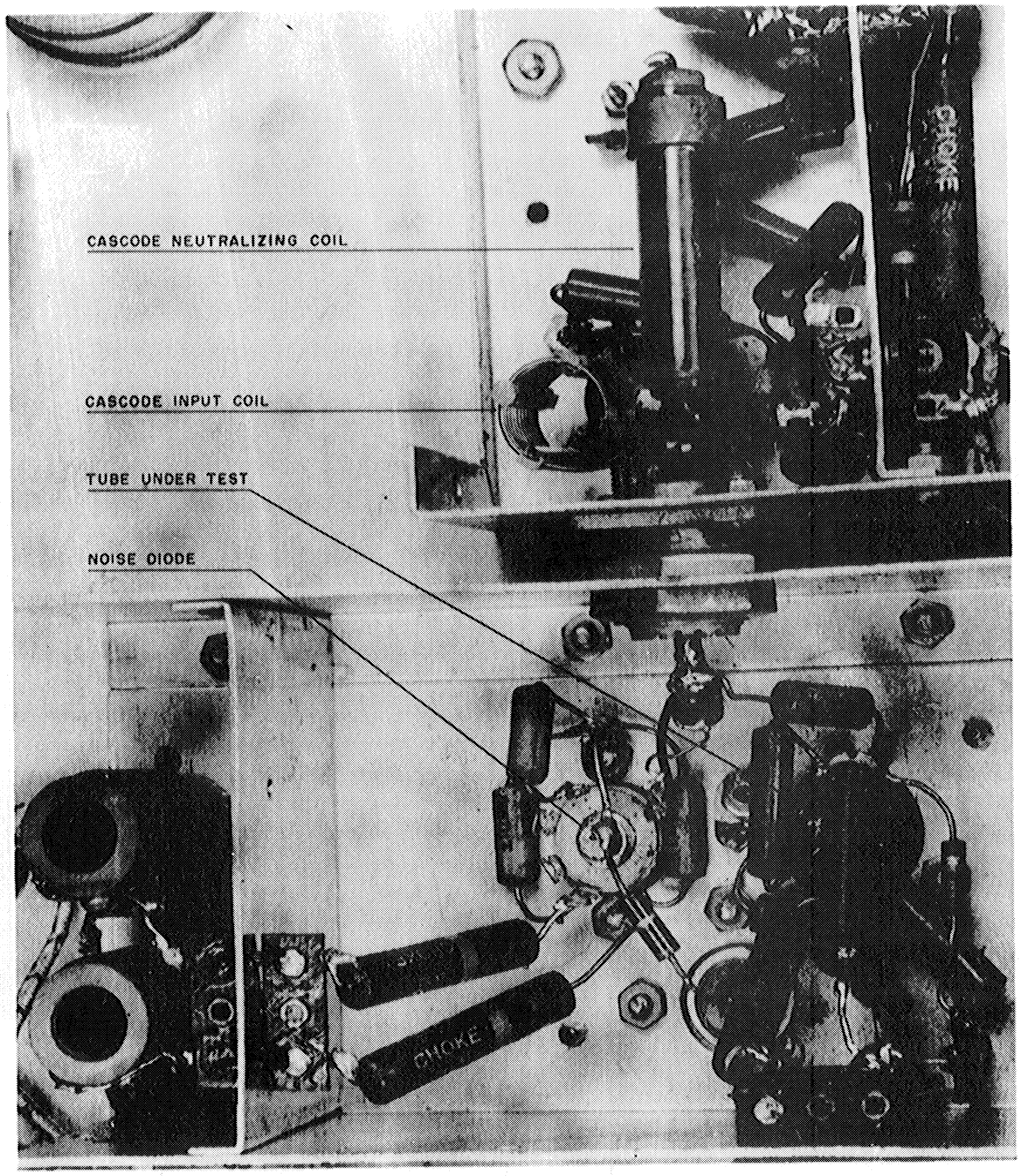

Figure 4.3. Photograph of the circuits of the cascode preamplifier input, the tube under test and the noise diode.

described below are also visible. The socket for the tube under test is mounted on a plate enabling it to be removed easily and replaced by a holder for a set of plug-in resistors for use in measuring the amplifier noise factor. Switches, controls and plugs for measuring currents and voltages are mounted on a larger chassis to which the two smaller ones shown in Fig. 4.3 are fastened.

The amplifier used for the noise measurements reported here consists of a cascode-input three-stage preamplifier coupled by a short coaxial link to a 30 mc. radar i.f. amplifier, modified slightly to make it more suitable for the present application. The circuits of the two components are shown in Fig. 4.4. Since most of the circuit is conventional, only certain details are pointed out here. References 2 and 6 contain excellent discussions on the design, construction and adjustment of amplifiers of this type and the reader is referred to these references for further information pertaining to the circuit details.

As indicated in Fig. 4.4 a small (ceramic) variable capacitor, C_t, is mounted in parallel with the input coil of the preamplifier. The sum of this capacitance, C_t, the capacitance of the tube under test and the capacitance of the preamplifier input circuit must be such as to resonate with the coil L_1. If the capacitance presented by the tube under test should change, then C_t will permit retuning the input circuit to the correct frequency.

The output of the preamplifier is coupled by a short length of coaxial cable to the input of the modified radar i.f. amplifier. Most of the r.f. plate current of the final stage of the preamplifier flows into this coaxial cable and through the 50-ohm resistor which terminates the cable. The voltage developed across this resistor is then used to excite the input tank of the i.f. amplifier. The use of coil L_5 , resonating with C_5 plus the input capacitance, provides a step-up in voltage from the coaxial input to the 6AK5 grid.

The gain of the amplifier is controlled by varying the grid bias of the second two 6AK5 stages. As the grid bias is varied on either of these tubes their input capacitance changes, detuning the input circuit (coil L_6 or L_7). To prevent this variation in input capacity, part of the cathode-bias resistor is left unby-passed. The amount of unby-passed resistance to be used, 47 ohms, was determined by trial and error, observing the change in resonant frequency of the input circuit as the gain control was varied.

In the development of Eq (1.7) for the measurement of induced grid noise it is necessary to assume that the bandwidth of the amplifier does not change when the tube under test is turned on and adds its input conductance to that of the cascode input circuit. In order to be certain that the bandwidth of the complete amplifier remains the same regardless of the loading of the input circuit, it is necessary to make the overall bandwidth of the amplifier less than one-half the bandwidth of the input circuit. With the input fed from a 50-ohm source the half-power bandwidth of the complete amplifier plus the detector circuit was found to be approximately 200 KC. Calculations showed that the bandwidth of the cascode input circuit is greater than 500 KC for all possible conditions of loading so that the assumption of constant amplifier bandwidth is justified.

The amplifier was carefully tested for evidences of regeneration since the presence of even a small amount of feedback to the input circuit of the amplifier would be detrimental to its noise factor. The importance of avoiding feedback coupling to the circuits of the tube under test and the noise diode has been pointed out previously, but it is mentioned again here for emphasis. On the other hand, regeneration within the amplifier itself, if it is not excessive, will have no disastrous effects on the measurement of noise from the tube under test since noise from this tube and noise from the comparator diode are affected identically by such regeneration. The amplifier was tested for regeneration (1) by the temporary application of plate voltages considerably higher than normal while advancing the gain control as far as possible and trying to detect a tendency for oscillation, (2) by observing the plate current of the first stages while varying the gain control, and (3) by trying to detect changes in the conductance of the input circuit as the gain control was advanced. After considerable time spent shielding components, adjusting by-passes, filtering leads to common supply voltages, etc., regeneration was finally eliminated or reduced to negligible proportions. Subsequent

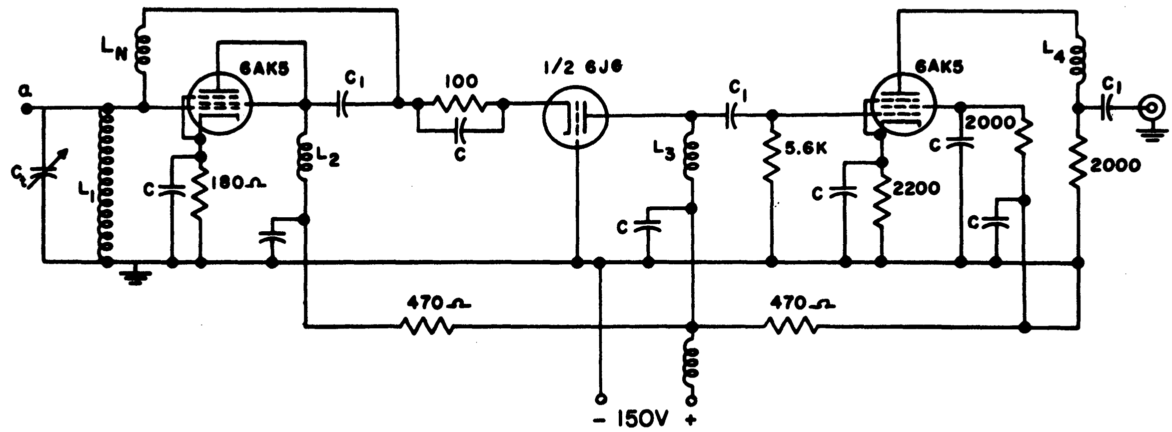

FIG. 4.4a

cascode preamplifier

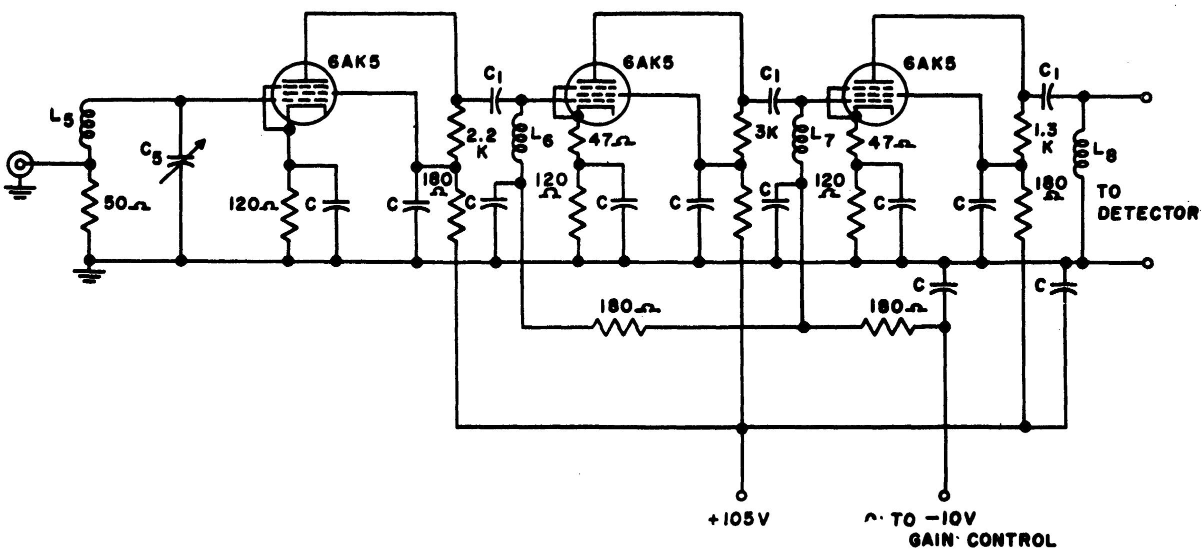

FIG. 4.4b

modified radar i.f. amplifier

measurements of the amplifier's noise factor bore out the conclusion of negligible regeneration by yielding results which were equal within experimental errors to the noise factor calculated from directly-measured values of grid and plate noise.

In the original radar i.f. amplifier the coil labeled L_8 in Fig. 4.4 was connected to the grid of the next 6AK5 stage. By designing an adapter which plugs into the socket of this stage a simple means was provided for obtaining an output connection from the amplifier. The detector, whose circuit is shown in Fig. 4.5, is actually built into this plug as close as possible to the amplifier output. The small 3.3 $\mu\mu$fd. capacitor in Fig. 4.5, together with stray capacitance, resonates with the coil L_8 in the amplifier, providing maximum signal for the detector.

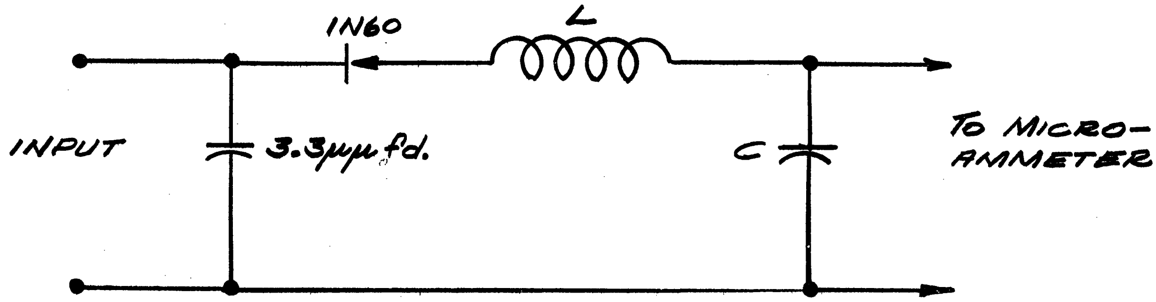

Figure 4.5. Circuit of the detector built into the adapter plug shown in Figure 4.6.

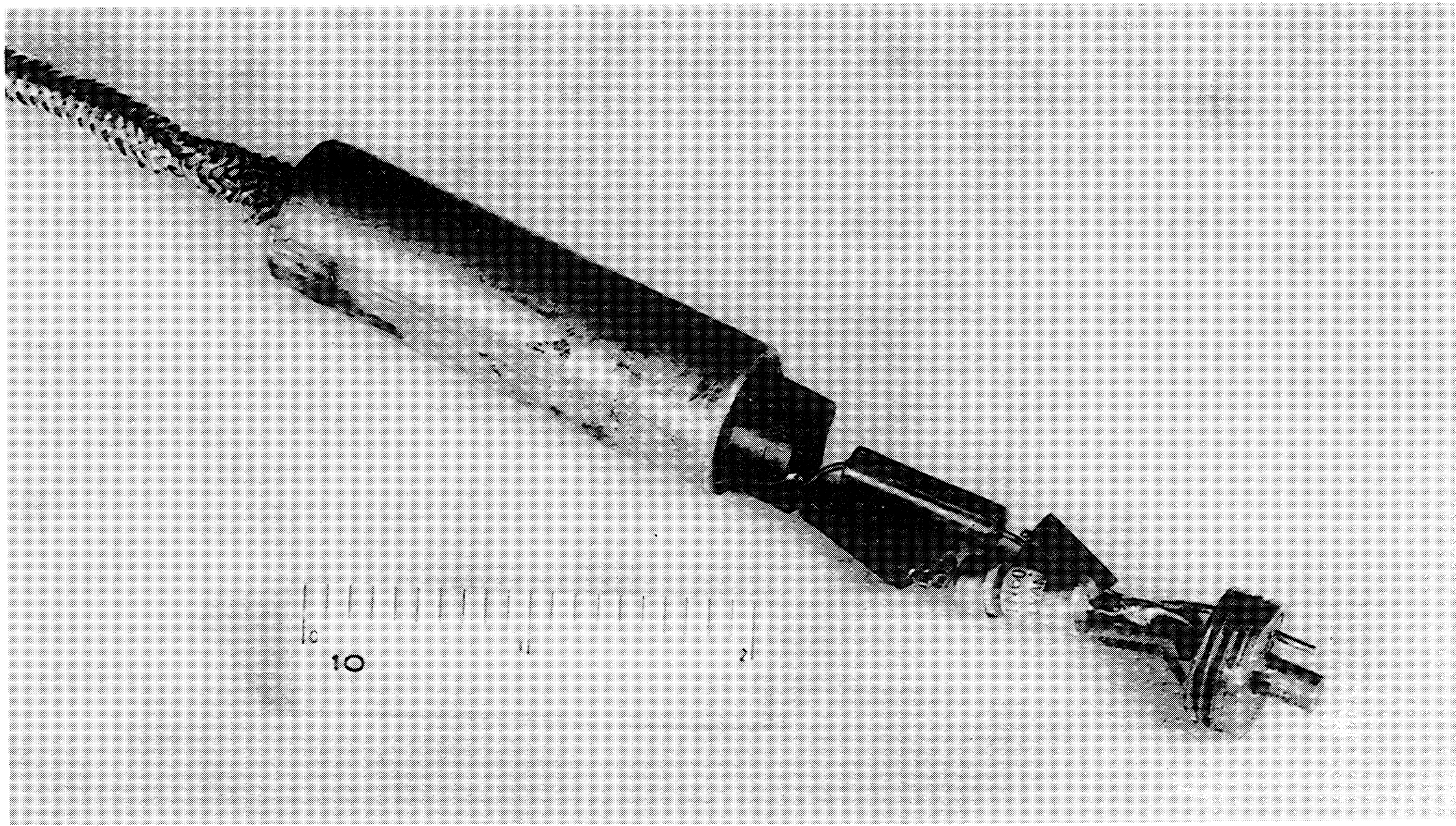

Figure 4.6. Photograph showing the mechanical construction of the detector built into the adapter plug. The scale is calibrated in inches.

Fig. 4.6 shows the mechanical construction of the adapter plug: two capacitors, a coil and the crystal fit inside a brass sleeve which is soldered to the end of a shielded cable leading to the microammeter. The large pin on the end of the plug fits as a guide into the center hole of a miniature socket, and the small pin fits as a tube prong into the proper socket contact.

The microammeter which is used as an output indicator is of a rather unusual type, consisting of a photoelectric tube mounted on a sensitive mirror galvanometer and connected in the feedback loop of a d.c. amplifier. Fig. 4.7 shows a photograph of the complete microammeter, including the galvanometer, phototube mount, amplifier, indicating meter and power supply. The sensitivity of this microammeter ranges from 0.5 to 10.0 microamperes full scale, depending on the position of the range switch. The advantages of this type of microammeter over an ordinary galvanometer are chiefly its rapid response and its extremely low input resistance. If the crystal detector is to have a good square -law response, it must operate into nearly a d.c. short-circuit and the device used here is ideally suited for such an application. The circuit described below has an input resistance of about 0.04 ohm.

The electrical circuit of the microammeter is shown in Fig. 4.8. It consists essentially of a modification of the circuit shown on page 490 of Reference 6, which also contains a discussion of the principle of operation of this type of feedback system. The modification embodied in the

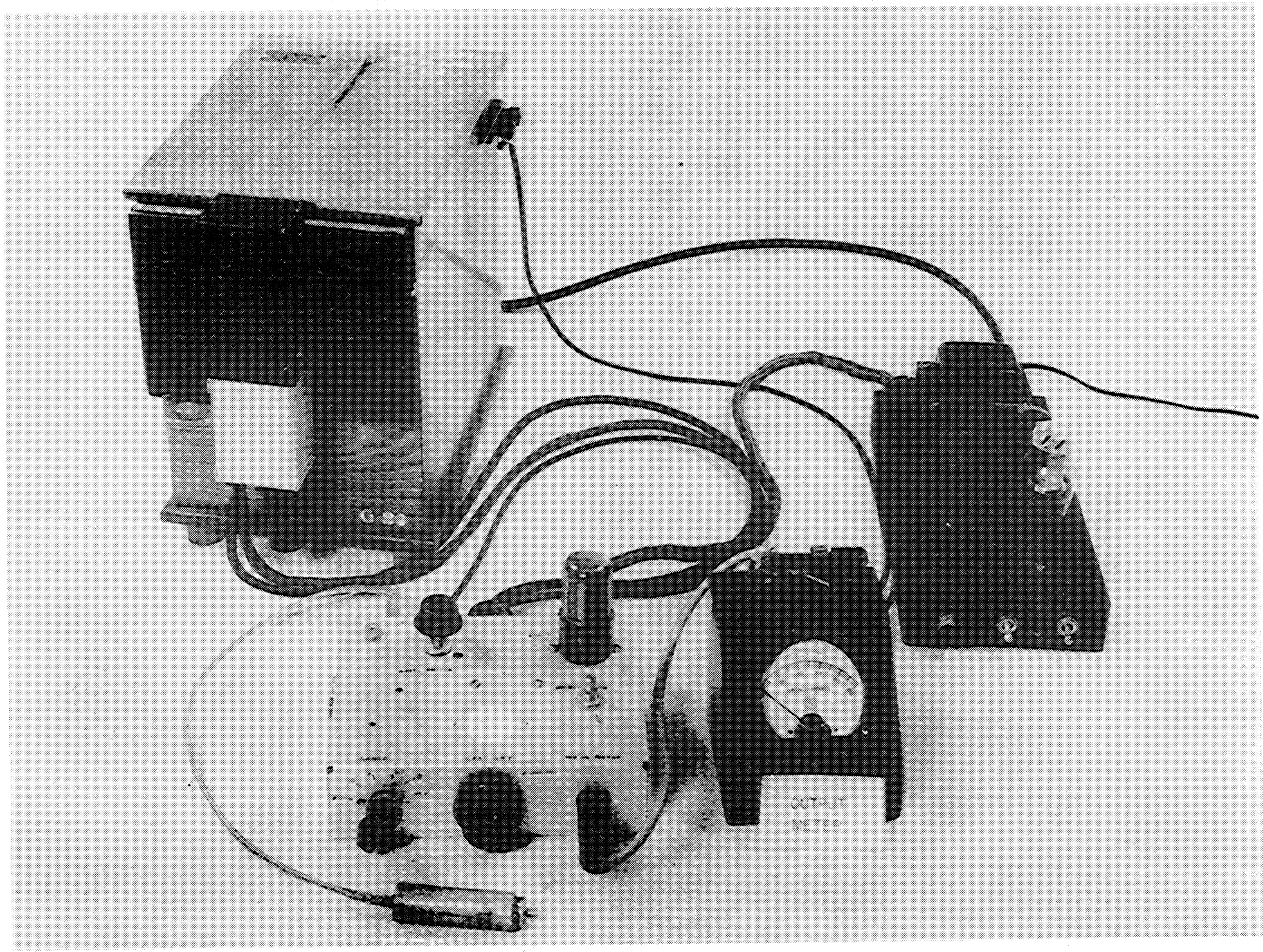

Figure 4.7. Photograph of the feedback microammeter. The phototube is mounted in the black box on the front of the galvanometer, and the 6SF5 is mounted (inverted) below it. The adapter plug containing the detector is visible in the foreground.

circuit of Fig. 4.8 consists of the addition of a cathode follower stage to supply the current for the feedback loop instead of obtaining this feedback directly from the plate circuit of the 6SF5. The additional stage was found necessary to insure good linearity for such a small full-scale current. The 929 phototube and the 6SF5 are mounted on the front of the galvanometer (see Fig. 4.7) and connected by a shielded cable to the remainder of the circuit.

The operation of the circuit of Fig. 4.8 is as follows: the introduction of a small current to the input terminals results in a current through the galvanometer coil and deflects the light spot which is focused on the photoelectric tube. The phototube is of the differential type and the deflection of the spot causes more light to fall on one cathode than on the other. This causes a change in the grid voltage of the 6SF5 and hence a change in its plate current. This current change is amplified by the cathode follower and a small portion, determined by the range switch, is fed back to the galvanometer coil and used to counteract the effect of the original input current. Thus the light spot is kept focused on the phototube and the amount of current which must be fed back to keep it there is a measure of the input current which produced the original unbalance.

The linearity of the complete system was tested by plotting a curve of output current as measured by the microammeter vs. the plate current of the temperature-limited diode. As discussed in Section 1.1 this plot should be a straight line if the amplifier is linear, if the crystal possesses a good square-law characteristic and if the microammeter is linear. That all of these conditions are satisfied for the apparatus

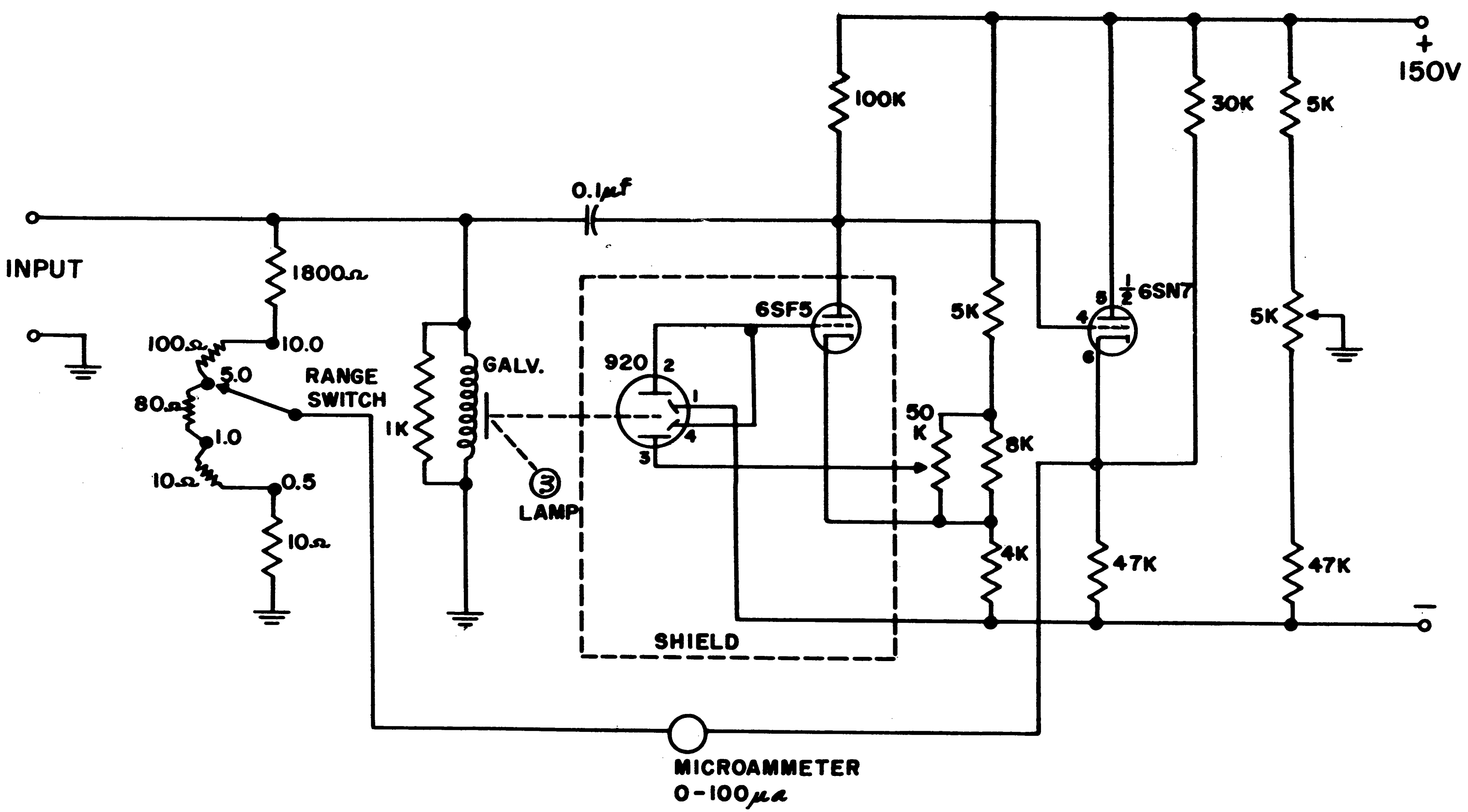

Figure 4.8. Circuit diagram of the feedback microammeter pictured in Figure 4.7.

employed here is clearly shown by Fig. 4.9.

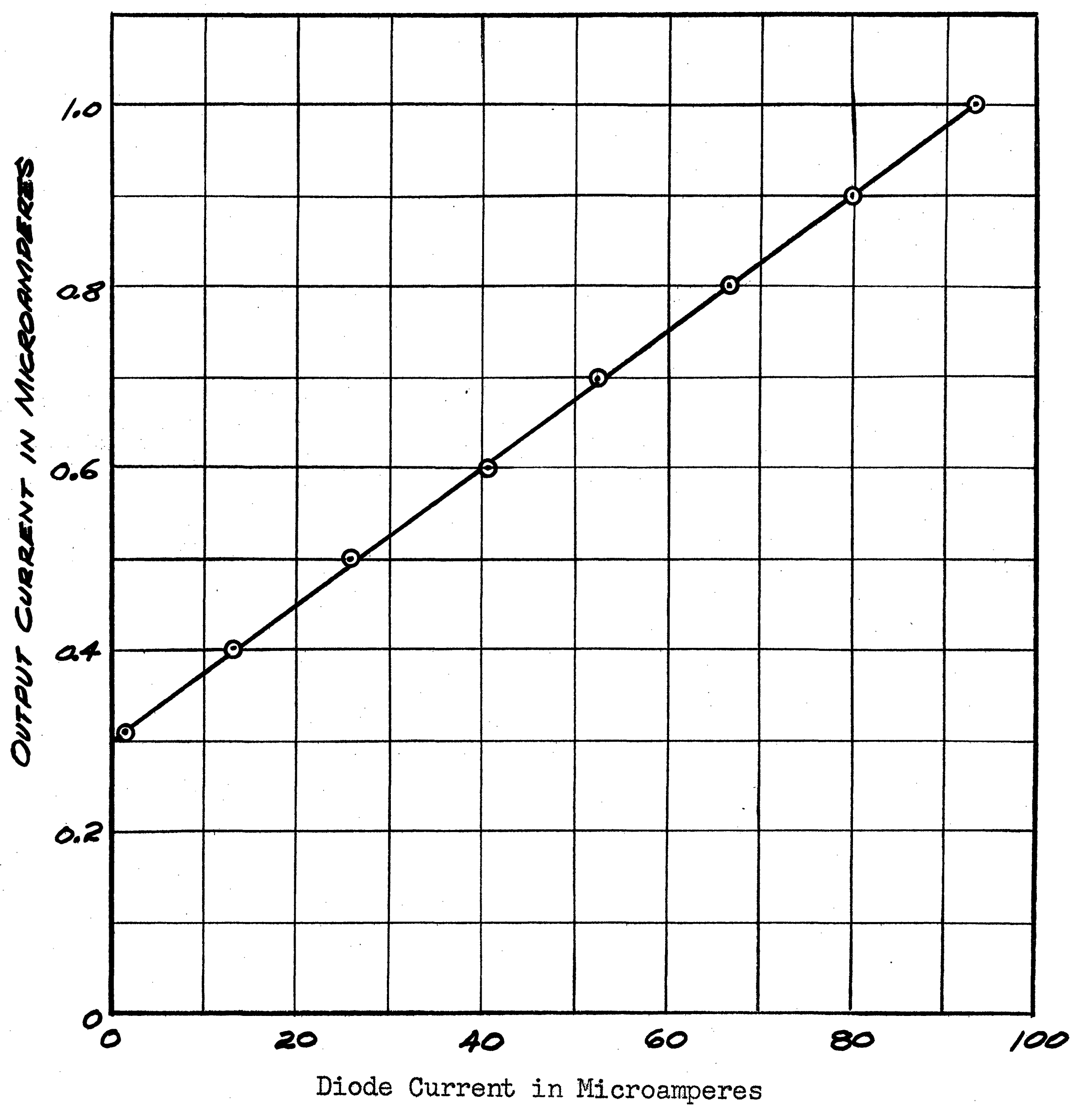

Figure 4.9. The results of a linearity test on the complete measuring apparatus. The microammeter output current is plotted as a function of the plate current of the temperature-limited diode.

5. Justification for Neglecting the Effect of Cathode Lead Inductance on Induced Grid Noise

The effect of inductance in the cathode lead can be quantitatively investigated by reference to Fig. 5.1. A current i_p is assumed to flow in the plate circuit and the grid current, i_g, produced by this plate current is calculated. The impedance of the tuned circuit connected to the grid is represented by R_g in Fig. 5.1, being a pure resistance when the circuit is in resonance as assumed here. The other symbols are self-explanatory.

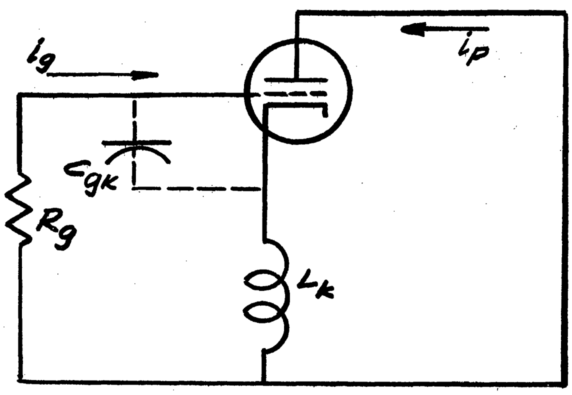

Figure 5.1. Equivalent circuit used to calculate the effects of cathode lead inductance.

Through the use of simple circuit theory it is easily shown that

$$i_g = \frac{\omega^2 C_{gk} L_k}{1 = j\omega C_{gk} R_g} \cdot ip \quad . \tag{5.1}$$

The largest that i_g could ever become is thus

$$i_g = \omega^2 C_{gk} I_k i_p \quad . \tag{5.2}$$

We proceed to calculate the mean square grid noise current produced through lead inductance effects by fluctuations in the plate current:

$$\overline{i_g^2} = (\omega^2 C_{gk} L_k)^2 \cdot \overline{i_p^2} \qquad (5.3)$$

Taking generous estimates of C_{gk} and L_k, for a 6AG5

$$C_{gk} = 6.5 \mu\mu \text{fd}$$
$$L_k = 0.01 \mu \text{hy}$$

we find that at a frequency of 30 mc.

$$\frac{\overline{i_g^2}}{\Delta f} = 2.5 \times 10^{-27} \text{ (amperes)}^2 \text{ per unit bandwidth.}$$

This is about one one-hundredth of measured grid noise values so that our assumption that grid noise produced by lead inductance effects is negligible seems completely justified.

An experimental check was also obtained using a 6J6 and inserting a piece of wire one inch long (Calculated to have an inductance of about 0.02μhy) in series with the cathode lead. No noticeable increase in grid noise could be detected.

BIBLIOGRAPHY

1. W. Schottky, "Spontaneous Current Fluctuations in Various Conductors", Ann. Physik, Vol. 57, pp. 541-567 (1918).

2. H. Wallman, A.B. Macnee, C. P. Gadsen, "A Low-Noise Amplifier", Proc. I.R.E., Vol. 36, pp. 700-708 (1948).

3. C. J. Bakker, "Fluctuations and Electron Inertia", Physica, Vol. 8, pp. 23-43 (1941).

4. E. J. Schremp, "Amplifier Sensitivity", Chapter 12, Vacuum Tube Amplifiers, Vol. 18, M.I.T. Rad. Lab. Series, McGraw-Hill, New York (1948).

5. D. O. North and W. R. Ferris, "Fluctuations Induced in Vacuum Tube Grids at High Frequencies", Proc. I.R.E., Vol. 29, pp. 49-50 (1941).

6. R. Q. Twiss and Y. Beers, "Minimal Noise Circuits", Chapter 13, Vacuum Tube Amplifiers, Vol. 18, M.I.T. Rad. Lab. Series, McGraw-Hill, New York (1948).

7. R. L. Bell, "Induced Grid Noise", Wireless Eng., Vol. 27, pp. 87-94 (1950).

8. S. Ballentine, "Schrot-effect in High Frequency Circuits", Jour. Franklin Inst., Vol. 206, pp. 159-167 (1937).

9. G. E. Duvall, "The Effects of Transit Angle on Shot Noise in Vacuum Tubes", M.I.T. Res. Lab. of Electronics, Tech. Rep. No. 82, Sept. 8, 1948.

10. E. Spenke, "Die Frequenzabhangigkeit der Schroteffektes", Wiss. Veroffent. Siemens-Werken, Vol. 16, pp. 127-136 (1937).

11. A. J. Rack, "Effect of Space Charge and Transit Time on the Shot Noise in Diodes", BSTJ, Vol. 17, pp. 592-619 (1938).

12. W. Schottky and E. Spenke, "Die Raumladungsschwächung des Schroteffektes", Wiss. Veroffent. Siemens-Werken, Vol. 16, pp. 1-41 (1937).

13. D. O. North, "Fluctuations in Space-Charge-Limited Currents at Moderately High Frequencies, Part II, Diodes and Negative Grid Triodes", RCA Rev., Vol. 4, pp. 441-472 and Vol. 5, pp. 106-124 (1940).

14. A. van der Ziel, "Fluctuation Phenomena", Advances in Electronics, Vol. 4, pp. 109-155, Academic Press (1952).

15. H. Nyquist, "Thermal Agitation of Electric Charge in Conductors", Phys. Rev., Vol. 32, pp. 110-113 (1928).

16. J. B. Johnson, "Thermal Agitation of Electricity in Conductors", Phys. Rev., Vol. 32, pp. 97-109 (1928).

17. B. J. Thompson, "Fluctuations in Space-Charge-Limited Currents at Moderately High Frequencies, Part I, General Survey", RCA Rev., Vol. 4, pp. 269-284 (1940).

18. F. C. Williams, "Fluctuation Voltages in Diodes and in Multi-electrode Valves", Jour. I.E.E., Vol. 79, pp. 349-360 (1936).

19. W. G. Dow, Fundamentals of Engineering Electronics, Second Edition, Wiley (1952).

20. F. B. Llewellyn and L. C. Peterson, "Vacuum Tube Networks", Proc. I.R.E., Vol. 32, pp. 144-166 (1944).

21. R. Kompfner, J. Hatton, E. E. Schneider and L. A. G. Dresel, "The Transmission-Line Diode as Noise Source at Centimetre Wavelengths", Jour. I.E.E., Vol. 93, Part III-A, pp. 1436-1442 (1946).

22. C. C. Cutler and C. F. Quate, "Experimental Verification of Space Charge and Transit Time Reduction of Noise in Electron Beams", Phys. Rev., Vol. 80, pp. 875-878 (1950).

23. J. R. Pierce, Travelling Wave Amplifiers, Van Nostrand, New York (1950).

24. A. van der Ziel, "Induced Grid Noise in Triodes", Wireless Eng., Vol. 28, pp. 226-227 (1951).

25. I. Langmuir, "The Effect of Space Charge and Initial Velocities on the Potential Distribution and Thermionic Current between Parallel Plane Electrodes", Phys. Rev., Vol. 21, pp. 419-435 (1923).

26. K. R. Spangenberg, Vacuum Tubes, McGraw-Hill, New York (1948).

27. P. H. J. A. Kleynen, "Extension of Langmuir's Tables for a Plane Diode with a Maxwellian Distribution of the Electrons", Philips Res. Rep., Vol. 1, pp. 81-96 (1945).

28. W. R. Ferris, "Input Resistance of Vacuum Tubes as Ultra-High-Frequency Amplifiers", Proc. I.R.E., Vol. 24, pp. 82-107 (1936).

29. D. O. North, "Analysis of the Effects of Space Charge on Grid Impedance", Proc. I.R.E., Vol. 24, pp. 108-136 (1936).

30. J. L. Lawson and G. E. Uhlenbeck, Threshold Signals, Vol. 24, M.I.T., Rad. Lab. Series, McGraw-Hill, New York (1950).

31. S. Goldman, Frequency Analysis, Modulation and Noise, McGraw-Hill, New York (1948).

32. D. B. Fraser, "Noise Spectrum of Temperature-Limited Diodes", Wireless Eng., Vol. 26, pp. 129-131 (1949).

33. S. O. Rice, "Mathematical Analysis of Random Noise", BSTJ, Vol. 23, pp. 282-332 (1944); Vol. 24, pp. 46-156 (1945).

34. T. C. Fry, Probability and its Engineering Uses, Van Nostrand, New York (1928).

35. N. R. Campbell, "Discontinuous Phenomena", Proc. Comb. Phil. Soc., Vol. 15, pp. 117-136 (1909); pp. 310-328 (1910).

36. E. A. Guillemin, The Mathematics of Circuit Analysis, John Wiley and Sons, New York (1949).

37. E. C. Titchmarsh, Introduction to the Theory of Fourier Integrals, Oxford Press, New York (1937).

38. A. van der Ziel, "Noise Suppression in Triode Amplifiers", Canad. Jour. Tech., Vol. 29, pp. 540-553 (1951).

39. M. J. O. Strutt and A. van der Ziel, "Verringerung der Wirkung Spontaner Schwänkungen in Verstärkern fur Meter-und Dezimeterwellen", Physica, Vol. 9, pp. 1003-1012 (1942); Vol. 10, pp. 823-826 (1943).

40. W. Kleen, "Verstärkung und Empfindlichkeit von UKW-und Dezimeter-Empfangsverstärkerröhren", Telefunken Rohre, Vol. 23, pp. 273-296 (1941).

41. A. Versnel and A. van der Ziel, "Induced Grid Noise and Total Emission Noise", Philips Res. Rept., Vol. 3, pp. 13-23 (1948).

42. R. L. Bell, "Negative Grid Partition Noise", Wireless Eng., Vol. 25, pp. 294-297 (1948).

43. K. G. McKay, "Secondary Electron Emission", Advances in Electronics, Vol. 1, pp. 65-130 (1948).

44. L. A. MacColl, "On the Reflection of Electrons by Metallic Crystals", BSTJ, Vol. 30, pp. 888-906 (1951).

45. H. E. Farnsworth, "Energy Distribution of Secondary Electrons from Copper, Iron, Nickel and Silver", Phys. Rev., Vol. 31, pp. 405-422 (1928).

46. C. Herring and M. H. Nichols, "Thermionic Emission", Rev. Mod. Phys., Vol. 21, pp. 185-270 (1949).

47. E. Rudberg, "Inelastic Scattering of Electrons from Solids", Phys., Rev., Vol. 50, pp. 138-150 (1936).

48. C. J. Davisson and L. H. Germer, "Diffraction of Electrons by a Crystal of Nickel", Phys. Rev., Vol. 30, pp. 705-740 (1927).

49. M. J. O. Strutt and A. van der Ziel, "The Causes for the Increase of the Admittances of Modern High-Frequency Amplifier Tubes on Short Waves", Proc. I.R.E., Vol. 26, pp. 1011-1032 (1938).

DISTRIBUTION LIST

15 Copies	M. Keiser Chief, Countermeasures Branch Evans Signal Laboratory Belmar, New Jersey
1 Copy	Prof. W. G. Dow Department of Electrical Engineering University of Michigan Ann Arbor, Michigan
1 Copy	H W. Welch, Jr. Engineering Research Institute University of Michigan Ann Arbor, Michigan
1 Copy	Document Room Willow Run Research Center University of Michigan Ann Arbor, Michigan
20 Copies	Electronic Defense Group Project File University of Michigan Ann Arbor, Michigan
1 Copy	Engineering Research Institute Project File University of Michigan Ann Arbor, Michigan